Journal of Cell Science 113, 3921-3930 (2000)
Printed in Great Britain © The Company of Biologists Limited 2000
JCS1690

Active protein transport through plastid tubules: velocity quantified by fluorescence correlation spectroscopy

Rainer H. Köhler[1,*], Petra Schwille[2,‡], Watt W. Webb[2] and Maureen R. Hanson[1,§]

[1]Department of Molecular Biology and Genetics and [2]School of Applied and Engineering Physics, Cornell University, Ithaca, NY, 14853, USA

*Present address: Lion Biosciences, 141 Portland Street, Cambridge, MA 02139, USA

‡Present address: Max-Planck-Institute for Biophysical Chemistry, 37077 Göttingen, Germany

§Author for correspondence (e-mail: mrh5@cornell.edu)

Accepted 27 August; published on WWW 31 October 2000

SUMMARY

Dynamic tubular projections emanate from plastids in certain cells of vascular plants and are especially prevalent in non-photosynthetic cells. Tubules sometimes connect two or more different plastids and can extend over long distances within a cell, observations that suggest that the tubules may function in distribution of molecules within, to and from plastids. In a new application of two-photon excitation (2PE) fluorescence correlation spectroscopy (FCS), we separated diffusion of fluorescent molecules from active transport in vivo. We quantified the velocities of diffusion versus active transport of green fluorescent protein (GFP) within plastid tubules and in the cytosol in vivo. GFP moves by 3-dimensional (3-D) diffusion both in the cytosol and plastid tubules, but diffusion in tubules is about 50 times and 100 times slower than in the cytosol and an aqueous solution, respectively. Unexpectedly larger GFP units within plastid tubules exhibited active transport with a velocity of about 0.12 μm/second. Active transport might play an important role in the long-distance distribution of large numbers of molecules within the highly viscous stroma of plastid tubules.

Key words: Active transport, Diffusion, Fluorescence correlation spectroscopy, Green fluorescent protein, Plastid tubule

INTRODUCTION

In addition to the intracellular compartments characteristic of all animal cells, plant cells have double-membrane-bound, genome-containing organelles termed plastids, whose characteristics vary depending on the cell type. Although fatty acids, amino acids and nucleotides are synthesized in the cytosol of animal cells, important steps in these biosynthetic processes occur in plastids in plant cells (reviewed in Dennis et al., 1997; Ohlrogge and Jaworski, 1997; Temple and Sengupta-Gopalan, 1997). Molecules synthesized in plastids must be distributed to the cytosol and to other organelles within the cell. Furthermore, molecules synthesized in other cellular compartments enter plastids to serve as substrates in a variety of metabolic processes (see Tobin, 1992). In addition, proteins encoded by the nuclear genome also traverse the plastid envelope membrane (reviewed in Keegstra and Cline, 1999; Fuks and Schnell, 1997), as the plastid genome encodes only a fraction of the proteins necessary for plastid function (Gillham, 1994).

Chloroplasts, the specialized type of plastid that contains chlorophyll and caries out photosynthesis, have long been regarded as oval-shaped, independent organelles present in large numbers in leaf cells. Expressing a plastid stroma-localized green fluorescent protein (GFP) in transgenic plants has provided new views of chloroplasts and of the non-green plastids present in other cell types (Köhler et al., 1997a). Thin tubular projections could be seen emanating from chloroplasts and occasionally connecting one chloroplast to another. The tubules are dynamic in living cells, and can be observed extending, retracting and moving within the cell. The abundance of tubules and appearance of plastids are tissue-specific and developmentally regulated (Köhler and Hanson, 2000). In certain non-green cells, virtually all plastids in a cell exhibit tubular extensions. In plant cells cultured in liquid (suspension cells), which are relatively large compared to most cells of the plant, the tubular projections are especially pronounced, often extending 40 μm toward the periphery of the cell (Köhler and Hanson, 2000). The tubular extensions and connections have been termed stromules for stroma-filled tubules (Köhler and Hanson, 2000). Two different plastid parts have been distinguished: stromules, plastid structures that appear less than 0.8 μm in diameter, and plastid bodies, larger parts of the plastid (Köhler and Hanson, 2000).

Stromules can serve as conduits between individual plastids. Photobleaching experiments revealed that GFP can flow from one plastid to another through an interconnecting stromule. Thus a plastid can acquire proteins and presumably other molecules from another plastid, in addition to the more well-characterized route through the selective envelope-membrane-associated import and export machinery. However, even in suspension cultured cells, where stromules are abundant, most

of the plastids appear to be independent. Optical sectioning as well as photobleaching experiments have revealed that most of the plastids within the cell are not interconnected (Köhler and Hanson, 2000). Therefore, transmission of molecules from one plastid to another is not likely to be the primary function of stromules. It remains possible, however, that stromules serve to distribute and to facilitate import and export of molecules to and from the plastid. Stromules appear to provide an indirect connection between the nucleus, which is surrounded by plastid bodies, and distant regions of the suspension cells (Köhler and Hanson, 2000).

Knowledge of the velocity of proteins moving through the stromules could be informative with respect to their possible role in intracellular and interplastid communication and distribution of molecules. Fluorescence correlation spectroscopy (FCS) is an extremely sensitive technique to derive information about particle concentration, motion and dynamics from fluctuating emission signals of small numbers of fluorescent molecules (Magde et al., 1972; Magde et al., 1974; Elson and Magde, 1974). For analysis of spontaneous fluctuations on a molecular scale, the system under observation must be restricted to low particle numbers, which is done by focusing the illuminating light down to ultra-small volume elements of less than 10^{-15} l (10 fl) in a confocal setup (Koppel et al., 1976). Two-photon excitation (2PE) with FCS provides sensitivity down to the single GFP molecule level and reduces problems such as light scattering, autofluorescence, photobleaching and photodamage (Schwille et al., 1999a).

Although FCS provides access to a large number of parameters such as local concentrations, translational and rotational diffusion and transport coefficients, rates of fast intramolecular and slow intermolecular dynamics, photophysical transitions, and particle aggregation (reviewed in Thompson, 1991), the majority of applications to date are concerned with analysis of particle mobility and, in particular, diffusion behavior (Schwille et al., 1997; Schwille et al., 1999a). The application of FCS for analysis of uniform translation (plug flow) and laminar flow has been established with theoretical derivations of particle motion dynamics by superimposed diffusion and active transport (Magde et al., 1978). An experimental validation was given for a dye system underlying laminar flow with a velocity distribution due to the Hagen-Poiseuille law. Since then, FCS flow analysis has been applied to analyze uniform flow in electroosmosis in electric fields of various strength in capillaries or on microstructures (Brinkmeier et al., 1999), but has not been employed to determine active transport behavior in living cells.

This study shows for the first time that FCS is capable of distinguishing between diffusion and flow modes of intracellular dynamics in vivo. By applying 2PE FCS, we have unexpectedly found that there is an active component to the molecular mobility of GFP in stromules, as well as self-diffusion. Diffusion of GFP through stromules is very slow compared to diffusion in the cytosol, which is about 100 times faster. The active component in the plastids can be inhibited by sodium cyanide (NaCN) or carbonyl cyanide p-(trifluoromethoxy)phenylhydrazone (FCCP), but returns after removal of the inhibitor. The passive diffusion-like motion, however, does not change upon drug addition. Although the velocity of the active transport component is small compared to the local diffusive motion, we conclude that the flow modus is more efficient for long distance transport of large quantities of molecules through stromules.

MATERIALS AND METHODS

Growth of plant material

Callus growth was induced by placing sterile leaf material from transgenic and wild-type tobacco plants (*Nicotiana tabacum, Petit havana*) kept in Magenta boxes onto NT1 agar medium (Köhler et al., 2000). Suspension cultures were grown in liquid NT1 medium, shaken at 110 rpm and transferred weekly to fresh NT1 medium. All cultures were grown under a 16 hours light:8 hours dark cycle at 25°C.

Vector construction

Cloning of the *35S35AMV-S65TmGFP4* and the *35S35S-CT-S65TmGFP4* construct and the transformation of tobacco *Petit havana* were done as described by Köhler et al. (Köhler et al., 1997a; Köhler et al., 1997b).

Imaging of plant material

Suspension cells were collected, treated with inhibitors and imaged 3-4 days after transfer to fresh NT1 medium while they were still in a logarithmic growth phase. Suspension cells were mounted on slides in liquid NT1 medium. Confocal laser scanning microscopy (CLSM) and light microscopy were done with a BioRad MRC-600 CLSM with a BHS filter cube (488DF10, Dichroic 510, Emission 515LP) and fiber optics and the COMOS program (BioRad, Hercules, CA, USA). GFP and light micrographs were imaged at the same time but saved as separate images. Image stacks taken along the optical *z*-axis in steps indicated in the figures were opened in Confocal Assistant 4.02 (Todd Clark Brelje, BioRad, Hercules, CA, USA) and projected into a single plane using maximum pixel value. For light micrographs, single images were selected that seemed to give the best representation of the general appearance of the cell including the nucleus, cytosolic strands and, if visible, plastid tubules.

Setup of the FCS

For fluorescence detection at a low scattering background and minimal interference with the cellular machinery, 2PE of GFP dye is used. A detailed discussion of FCS applications with 2PE and a scheme of the experimental apparatus used is given elsewhere (Schwille et al., 1999a). FCS is carried out with a modified Zeiss IM-35 inverted microscope using the camera port for confocal FCS detection. The 2PE is performed by epi-illumination of a Nikon 63×1.2 NA water immersion objective by the parallel beam of a mode-locked tunable Spectra Physics (Mountain View, CA, USA) Tsunami Titanium-Sapphire laser with 80 MHz, 100 fs pulse width. The objective back aperture is slightly overfilled, creating a diffraction-limited focal spot. The effective focal measurement volume defined by 2PE is about 10^{-16} l in size with a lateral diameter of about 0.9 μm and a structure parameter r_0/z_0=3.5 (see below) determined in calibration measurements. It is imaged by the 160 mm tube lens onto the 100 mm diameter core opening of a multimode optical fiber (OZ optics, Carp, Canada), connected to a single-photon counting avalanche photodiode (EG&G SPCM-200 FC). The GFP mutant S65TMGFP4 is excited at the two-photon absorption maximum at 920 nm. The detector signal is correlated online by the ALV-5000E correlator board (ALV, Langen, Germany). The laser intensity is chosen between 0.5 and 5 mW to avoid bleaching of the dye and photostress or photodamage of the cells.

FCS correlation curves, diffusion coefficients and velocities

Correlation curves for GFP in aqueous solution or in the cytosol of tobacco cells are represented as single measurements because their

standard deviation was negligible. All other curves are averages of ten successive measurements, each 10-30 seconds long. Diffusion coefficients and velocities were calculated by averaging the fitting results from 10-30 FCS curves, each derived from ten successive measurements. Different FCS curves were obtained from cells taken from at least three different Erlenmeyer flasks at different times.

Theory of molecule movement

The normalized fluorescence fluctuation autocorrelation function $G(\tau)$ for a fluorescence signal $F(t)$ of a molecular system at mean concentration $\langle C\rangle$ in a fixed illuminated measurement volume V with average values $\langle F\rangle \propto V\times\langle C\rangle$ is given by:

$$G(\tau)=\langle \delta F(t)\delta F(t+\tau)\rangle/\langle F\rangle^2, \quad (1)$$

and corresponds to the probability for a fluorescent particle that was inside this volume at time t to be still inside at time $(t+\tau)$. $G(\tau)$ is the convolution of the so-called concentration correlation factor $\phi=\langle \delta C(\underline{r}(t+\tau))\delta C(\underline{r},t)\rangle$ with the spatial distribution of illumination intensity $I(r)$ (Elson and Magde, 1974). If the particle motion is composed of diffusion with diffusion coefficient D and uniform active transport (plug flow) with velocity v, with the y axis being oriented along the flow direction, the following 3-D correlation factor is obtained (following Magde et al., 1978):

$$\phi(\underline{r},\underline{r}',\tau)=\frac{1}{(4\pi D\tau)^{3/2}}\exp\left(\frac{-(x-x')^2-(y-y'-v\tau)^2-(z-z')^2}{4D\tau}\right).$$

Assuming Gaussian intensity distribution in all directions with $1/e^2$ half-axes r_0 and z_0: $I^2(\underline{r})=I_0^2\exp(-4r^2/r_0^2-4z^2/z_0^2)$ for 2PE (Schwille et al., 1999a), $G(\tau)$ can be calculated as follows:

$$G(\tau)=\frac{1}{N}\times\frac{1}{1+\tau/\tau_d}\sqrt{\frac{1}{1+(r_0/z_0)^2\tau/\tau_d}}\exp\left(-\left(\frac{\tau}{\tau_f}\right)^2\times\frac{1}{1+\tau/\tau_d}\right). \quad (3)$$

N is the average number in the focal detection volume and $\tau_d=r_0^2/8D$, the average residence time of particles if there was only diffusion. In contrast, $\tau_f=r_0/v\sqrt{2}$ is the average residence time if there was only active transport. The two limiting cases, diffusion only for $\tau_f\rightarrow\infty$, and transport only for $\tau_d\rightarrow\infty$, can be derived easily from equation 3:

$$\text{diffusion:}\quad G_{Diff}(\tau)=\frac{1}{N}\times\frac{1}{1+\tau/\tau_d}\times\sqrt{\frac{1}{1+(r_0/z_0)^2\tau/\tau_d}}, \quad (4)$$

$$\text{flow:}\quad G_{Flow}(\tau)=\frac{1}{N}\times\exp-\left(\frac{\tau}{\tau_f}\right)^2. \quad (5)$$

If the diffusion is not strictly Brownian but anomalous, due to particle interaction with fixed or mobile structures, equation 4 has to be modified as follows (Schwille et al., 1999b):

$$G_{Anom}(\tau)=\frac{1}{N}\times\frac{1}{1+(\tau/\tau_{d,a})^\alpha}\times\sqrt{\frac{1}{1+(r_0/z_0)^2(\tau/\tau_{d,a})^\alpha}} \quad (4A)$$

where α is the exponent of the mean square displacement time dependence: $\langle\Delta r^2\rangle\sim t^\alpha$ determines the degree of restriction, and $\tau_{d,a}$ is again the characteristic residence time. A restriction coefficient of $\alpha=1$ is normal; the smaller α, the more restricted (or anomalous) the diffusion behavior.

Treatment with inhibitors

A 3-4 day old suspension culture was separated into 5 ml portions into 25 ml Erlenmeyer flasks. The portions were shaken at 110 rpm at 25°C in a growth room until samples were taken. To deplete cells of ATP, a 100 mM stock solution of NaCN (Sigma, St Louis, MO, USA) in NT1, or a 1 mM stock solution of FCCP (Sigma, St Louis, MO, USA) in 95% ethanol, were added to a final concentration of 1 mM NaCN or 1 μM FCCP, respectively. Cells were imaged within 30-120 minutes of sampling. To remove the inhibitors the suspension cells were washed four times in 45 ml of NT1 medium. Suspension cultures were transferred to sterile 50 ml centrifuge tubes, mixed with 45 ml NT1 medium, and centrifuged at 2000 ***g*** for 10 minutes at 25°C. After removal of the supernatant the pellet was resuspended in 45 ml of NT1 and the washing was repeated three more times. Finally the suspension cells were transferred to a new flask and shaken until used.

Release of GFP from plastids and the cytosol

Suspension cells were collected in Eppendorf tubes and centrifuged at 5000 rpm (1400 ***g***) for 10 minutes at room temperature. The supernatant was removed and the pellet frozen at –80°C. The frozen cells were thawed, an equal volume of 100 mM Tris/HCl buffer, pH 7.6, was added, and the cells were ground with Kontess pestles (Kontess, Vineland, NJ, USA) and a drill. Broken cells and soluble proteins were then separated by centrifugation at 13000 rpm (9500 ***g***) for 15 minutes. The supernatant was removed and used for FCS measurements.

RESULTS

Localization of GFP in the plastid stroma and cytosol

The fluorescence-enhanced and plastid-targeted GFP that we utilized, CT-S65TMGFP4, is predicted to contain 15 additional amino acids (AKKLSHKISSGFDRD) of the mature RECA protein at its N terminus after import from the cytosol and processing (Cerutti et al., 1992; Cao et al., 1997; Haseloff et al., 1997; Köhler et al., 1997a). CT-S65TMGFP4 appears to be evenly distributed in the plastid stroma of tobacco suspension cells, except that it is excluded from some areas that might be thylakoid membranes and/or inclusions such as starch grains, oil, or protein bodies (Figs 1A,B, 2; Köhler et al., 1997a). Exclusion of GFP from an area or compartment is visible by the absence of any green fluorescence. GFP without a localization signal is unable to penetrate membranes and cannot enter compartments that are enclosed in membranes such as plastids, mitochondria or the ER, unless it is fused to a transit peptide. Nuclear-encoded expression of GFP lacking a transit peptide leads to fluorescence in the cytosol and nucleus (Fig. 1C,D). Cytosolic GFP enters and leaves the nucleus by diffusion through the nuclear pore complex (Grebenok et al., 1997; Köhler et al., 1997b; Köhler, 1998). Similar to GFP in the stroma, cytosolic GFP appears to be evenly distributed except for exclusion from membrane-bound compartments other than the nucleus. The relatively homogenous distribution of GFP in the stroma and the cytosol implies that GFP does not have strong affinity to particular subcellular structures and is not restricted to inclusion bodies. In addition, GFP is rapidly released from broken cells or broken plastids (data not shown; Köhler et al., 1997a) and can be observed to move through stromules and the cytosol of plants following photobleaching of individual plastids or of small regions within the cell (data not shown; Köhler et al., 1997a; Köhler and Hanson, 2000).

Measurement volume for FCS

We used 2PE for FCS because it yields a better signal-to-noise ratio in the cellular environment, reduces photobleaching, and causes less background fluorescence, and has fewer negative effects on the exposed cells than single-laser excitation,

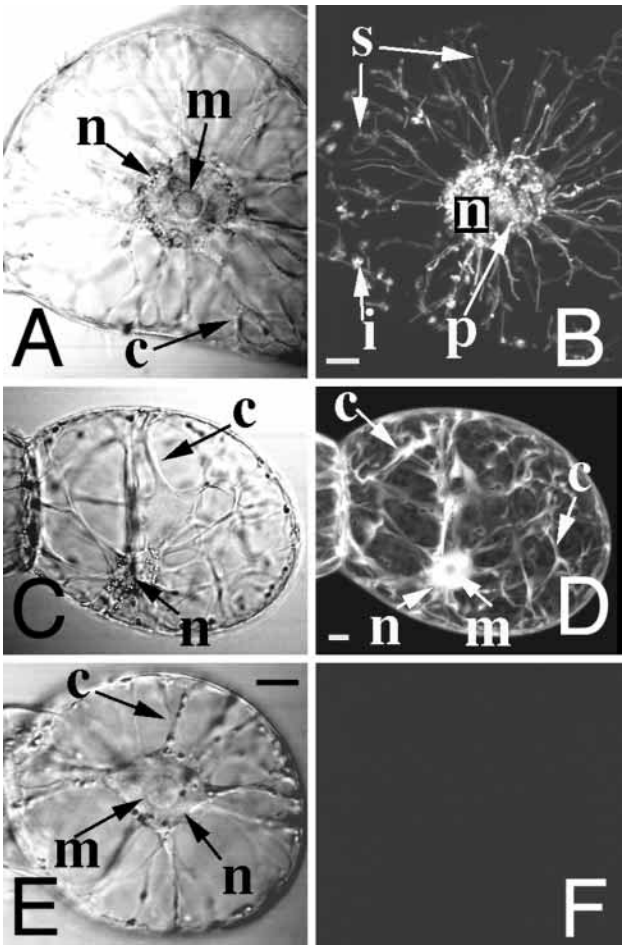

Fig. 1. Micrographs of tobacco suspension cells with GFP-labeled cytosol or plastids. (A,C,E) Single light microscopic images of suspension cells. (B,D,F) CLSM images of the same cells. The CLSM images are projections of *z*-stacks collected along the optical *z*-axis at 0.5 μm intervals. The number of images projected into a single plane is indicated in parentheses. (A,B) Plastid-targeted CT-S65TMGFP4 (91 images); (C,D) cytosol-localized S65TMGFP4 (78 images); (E,F) non-transgenic control cell (70 images); c, cytoplasmic strand; i, non-fluorescent inclusion; m, nucleolus; n, nucleus; p, plastid bodies around the nucleus; s, stromule. Bars, 10 μm.

because excitation is limited to the direct vicinity of the focus (Schwille et al., 1999a). In contrast to confocal laser scanning microscopy (CLSM), which scans the sample to collect a complete image, the excitation for FCS is stationary and restricted to a single location, so that the measurement volume appears as a single fluorescent spot when observed by light microscopy (Fig. 2A). In cells with GFP in the plastid stroma, green fluorescence emission and an FCS signal for GFP was only observable when the laser beam was focused onto areas that contained plastid stroma. Other areas of the cell did not show significant fluorescence emission and did not give a correlated signal.

Mobility of GFP in the cytosol

Before initiating studies on stroma-localized GFP, we determined the diffusive mobility of our particular modified GFP, S65TMGFP4, in the cytosol of tobacco cells and in a buffered aqueous solution. The diffusion coefficients of different GFP mutants in the cytosol of RBL 2H3 cells vary by a factor of 10 between mutants; for example, the cycle 3 mutant and wild-type GFP exhibit diffusive mobilities of 4.3×10^{-7} cm^2/second and 0.4×10^{-7} cm^2/second, respectively (Yokoe and Meyer, 1996). The slow diffusion of wild-type GFP might be the result of hydrophobicity and self-aggregation, as has been suggested by Crameri et al. (1996). A comparison of the recorded FCS correlation curves obtained by analysis of S65TMGFP4 is given in Fig. 3. Fitting the curves with different mathematical models for diffusion (equation 4) and/or active transport (equations 3 and 5) shows that S65TMGFP4 exhibits pure normal (Brownian) diffusion with no active transport contributions in aqueous solution or in the cytosol (Fig. 3).

Calibration of the measurement volume geometry with a dye of known diffusion properties enabled us to determine the diffusion coefficients of the GFP molecules from the FCS curves, as described elsewhere (Schwille et al., 1999a). The measured diffusion coefficient of S65TMGFP4 in the cytosol of tobacco is $4\pm2\times10^{-7}$ cm^2/second, about 2-3 times smaller than the diffusion coefficient of S65TMGFP4 in the aqueous solution, which is about $9\pm2\times10^{-7}$ cm^2/second. Slower diffusion is visible as a shift of the correlation curve to larger τ. τ_d represents the average time that GFP molecules need to move through the measurement volume. Additional information about GFP concentration is given by the correlation amplitude G(0), which is the reciprocal of the average number of particles (*N*) in the measurement volume (see Materials and Methods). We obtained numbers *N* of 50-500, corresponding to molecular concentrations of approximately 100 nM to 1 μM (determined as described by Schwille et al., 1999a).

GFP mobility in stromules

The majority of transgenic suspension cells and all cells measured by FCS had the plastid and stromule structure shown in Figs 1A, 2B. The measurement volumes, as illustrated in Fig. 2B, were located on the long thin stromule portions of plastids. If the measurement volume was placed within a plastid stromule, the fluorescence signal alternated between relatively dim periods with small and fast fluctuations (t[small&fast]), and bright periods with very large and slow fluctuations (Fig. 4A). The average fluorescence intensity during the slow fluctuations can be about 10-100 times higher in peaks than during dim periods. Although the periods of large fluctuations are interrupted by long (several tens of seconds) dim periods, their contributions dominate overall FCS correlation curves (Fig. 4A,B curve 2) because of their high brightness. The overall curves cannot be fitted to equation 4, which describes pure normal or restricted diffusion, nor to equation 5, which describes pure active transport (Fig. 5). Nevertheless, the data can convincingly be fitted by assuming a mixed motion composed of diffusive and transport-like elements, following the model of plug flow (Magde et al., 1978) given by equation 3. This indicates that the periods of large fluctuations are due to batches of GFP with high brightness in diffusion and active movement through the volume; these periods are separated by comparably ‘silent’ or dim periods with small and fast fluctuations caused by movement of single GFP molecules only. Due to the very slow

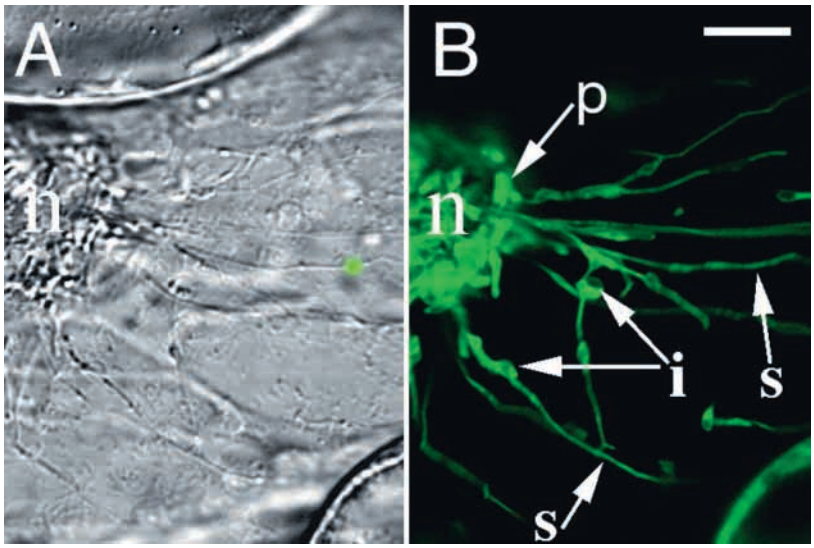

Fig. 2. Appearance of suspension cells and stromules in CLSM or FCS. (B) Single CLSM micrograph of a cell expressing GFP localized to plastids. (A) Single light microscopic image of the same cell with the green spot indicating the point of excitation of the laser as it appears in FCS. i, non-fluorescent inclusion; n, nucleus; p, plastid body; s, stromule. Bar, 10 μm.

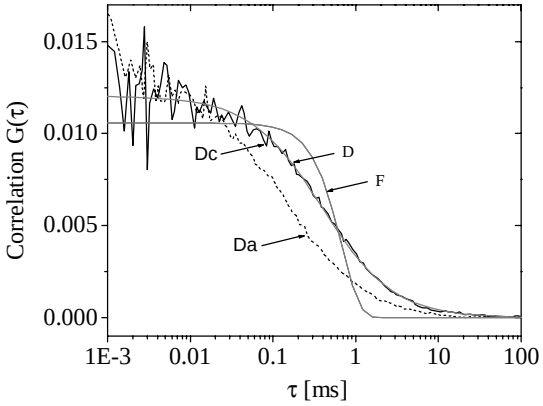

Fig. 3. GFP movement in the cytosol and in buffer. Fluorescence correlation curves of S65TMGFP4 in the cytosol of tobacco cells (solid line, Dc) and in an aqueous buffer (dotted line, Da; 100 mM Tris/HCl, pH 7.6) compared and fitted to the models for pure 3-D diffusion (D) and pure active transport (F).

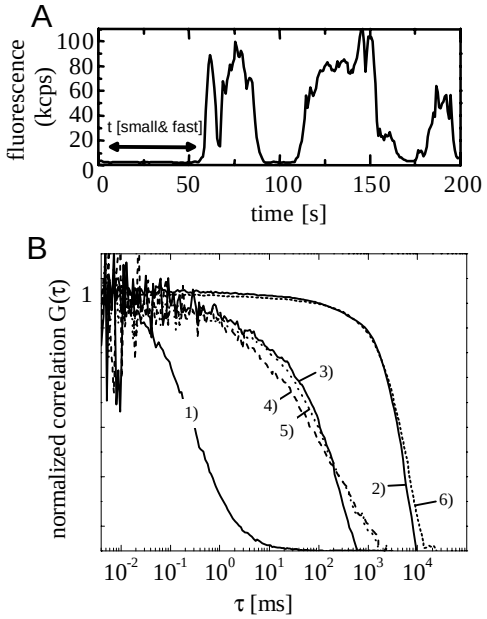

Fig. 4. Movement of GFP in plastid tubules. (A) Average fluorescence count rate in kilo counts per second (kcps) when the focal spot is placed in a stromule; (B) fluorescence correlation curves of GFP in stromules of tobacco suspension cells compared to results from GFP in the cytosol. (1) Cytosol; (2) stromule from an untreated cell that shows active transport and diffusion (see Fig. 5); (3) data restricted to dim periods with small and fast fluorescence fluctuations of a stromule, when no active transport occurs (see A); (4,5) stromule in a cell treated with NaCN or FCCP, respectively; (6) stromule in a cell treated with NaCN but after the inhibitor has been removed. The curves are normalized to the same G(0) in order to better compare their temporal progression.

changes in fluorescence during the periods of active transport, the variance in the overall correlation curves is rather high, up to 50%. In the majority of measurements, the actively transported batches of GFP need between 2000 and 6000 ms to move through the sample volume (Fig. 4, curve 2) which corresponds to transport velocities of 0.12±0.06 μm/second. Occasionally, values above 0.4 μm/second or below 0.03 μm/second have been measured. In addition to this dominant active transport, a very small diffusion coefficient for the GFP batches could be determined, with average values in the order of 10^{-11} cm^2/second.

In order to access the mobility parameters of single GFP molecules during dim periods that show small but fast fluctuations of fluorescence, we restricted the data recording to intervals between the periods of large fluctuations that otherwise dominate the curves (Fig. 4A,B, curve 3). The correlation curves for these dim periods fit well with equation 4A, which represents a pure 3-D diffusion model without active transport components. The diffusion, however, is anomalous with a restriction coefficient $\alpha \approx 0.5$ (Feder et al., 1996; Brown et al., 1999; Schwille et al., 1999a; Schwille et al., 1999b), which describes a degree of evanescent attractive interaction between molecules that preferentially slows diffusive transport over longer distance and times. The diffusivity can be approximated by a 3-D diffusion coefficient of $9\pm5\times10^{-9}$ cm^2/second. It is about 100 times lower than the diffusion coefficient of GFP in aqueous solution of $9\pm2\times10^{-7}$

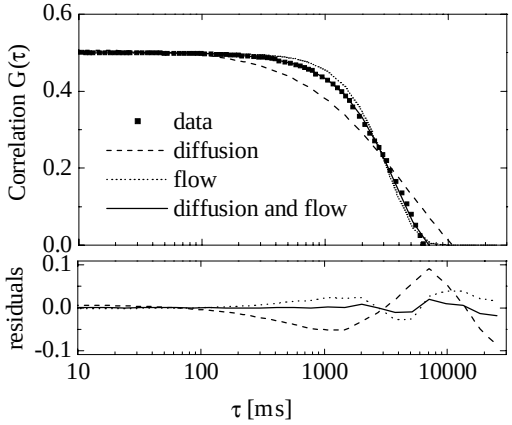

Fig. 5. Stromule GFP moves by active transport and slow diffusion. (Top) Correlation curve of GFP in plastid tubules (the corresponding fluorescence traces are shown in Fig. 4) compared with and fitted to different mathematical models for movement of molecules. Squares, measurement of GFP in plastid tubules; dashed line, fit by free 3-D diffusion (τ_d=4800 ms); dotted line, fit by pure active transport (τ_f=3300 ms), solid line, diffusion and flow model (τ_d=14 800 ms, τ_f=3700 ms). (Bottom) Fit residues; deviation of the fitted curves of the models for diffusion (dashed line), active transport (dotted line), and the mixed model for active transport and diffusion (solid line) from the data obtained in stromules. The model for a mixed movement of diffusion and active transport shows the smallest deviation.

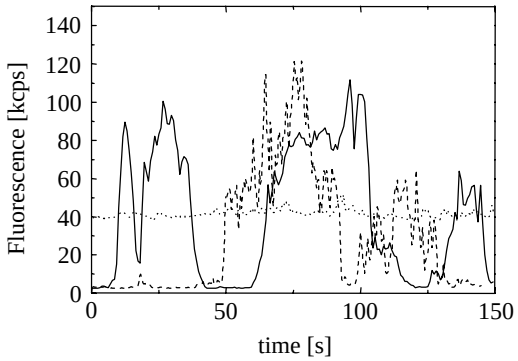

Fig. 6. Reversible inhibition of active GFP transport. Fluorescence fluctuations in stromules of suspension cells treated with NaCN (dotted line) compared to untreated cells (black solid line) and cells treated with NaCN but after removal of the inhibitor through washing with NT1 buffer (dashed line). Shown is the average fluorescence count rate in kilo counts per second (kcps) when the focal spot is placed into a stromule.

cm^2/second. Stromal GFP diffusion is therefore in the order of membrane-bound protein diffusion, which is around 10^{-8} cm^2/second. However, the correlation curves cannot be fitted assuming 2-D Brownian motion, as it would be expected for the 2-D diffusion of membrane-bound proteins (Schwille et al., 1999a; Schwille et al., 1999b). In contrast, the curves fit the 3-D diffusion model, suggesting that GFP exists in the stroma as a soluble molecule that can diffuse in three dimensions. The 3-D anomalous or restricted diffusion with values of alpha smaller than one indicates that the GFP interacts with intratubular structures or large molecules inhibiting its diffusion. Active transport can be seen only during the periods of large intensity fluctuations.

In summary, GFP moves through stromules in two different fashions, by continuous non-directional diffusion in three dimensions and by slow 'pulsed' active transport in large units (batches). The units themselves are about 10- to 100-fold brighter than the background from single GFP molecules and exhibit a small additional diffusional contribution with a diffusion coefficient two orders of magnitude smaller than for the 'free' GFP. As known from FCS theory (Magde et al., 1972), the correlation amplitude G(0) is determined by the frequency and relative strength of signal fluctuations. Fluctuations during the dim periods are due to individual GFP molecule movements. The overall curves are dominated by the large fluctuations and yield information about concentration and mobility of the large batches only.

From the G(0) values of overall correlation curves and of the curves recorded exclusively during the dim periods, rough estimates of the concentrations of GFP batches as well as of free GFP can thus be given (data not shown). With G(0)≈0.01 in dim intervals, we approximate the concentration of free GFP to be of the order of 200 nM, whereas G(0) of the overall curves yields values up to 1-2, indicating that the concentration of batches is at least 100-fold smaller. Information about GFP concentration within the batches themselves cannot be obtained from the G(0) values. However, the fact that the batches are much brighter than the background GFP suggests that they contain high local GFP concentrations.

Active transport of GFP can be reversibly inhibited

If, as predicted by modeling of the FCS data, GFP moves through stromules by an active transport process as well as by diffusion, then the active process should be inhibitable by cellular poisons. In order to separate the active transport from diffusion, cells were treated with two different non-specific inhibitors, NaCN and FCCP. Cyanide competes with oxygen for subunit III of cytochrome oxidase and inhibits the electron transport chain (Tzagoloff, 1982). FCCP is an ionophore that transfers protons (H^+) across membranes and dissipates membrane potentials (Heytler and Prichard, 1962). Both inhibitors deplete cells of ATP and interrupt active processes. The influences of the inhibitors on cytoplasmic streaming and on the growth of the suspension cultures were monitored to verify that the inhibitors entered the cells and inhibited ATP production. Both inhibitors produced the same visible and growth effects in all experiments. 30 minutes after addition of 1 mM NaCN or 1 μm FCCP, cytoplasmic streaming had stopped (data not shown). In addition, the growth of the cultures ceased, as monitored by the change in optical density at 600 nm (data not shown). Neither NaCN nor FCCP had an influence on the appearance of the stromules observed by CLSM or the shape of the cells visible by light microscopy when incubated for up to 3 hours (data not shown). Cells treated with NaCN or FCCP showed the same results in FCS; they lost the FCS signal representing the large and slow intensity fluctuations seen in Fig. 4A that fit the mathematical model for the active transport (Fig. 6). Only an almost constant intensity signal remained. The correlation curves after addition of the inhibitors (Fig. 4, curves 4 and 5) exhibit the same temporal progression as the ones measured during the dim intervals of small and fast fluctuations in untreated cells (Fig.

4, curve 3). The average amplitudes G(0) are somewhat lower, however, indicating that the concentration of free GFP is increased. The curves can be described assuming pure 3-D diffusion without active transport contributions, with an average diffusion coefficient in the same range as determined for the free GFP during the dim periods, of $9\pm5\times10^{-9}$ cm^2/second. Like diffusion without inhibitors, the diffusion in the presence of the inhibitors is restricted, with values of $\alpha\approx0.5$-0.6.

The inhibition of the active transport component of GFP movement through stromules is not a result of permanent cell or stromule damage caused by the inhibitors. After removal of NaCN by washing the cells several times in NT1 medium, the periods of high fluorescence with large and slow fluctuations characterized as flow-like transport appeared again (Fig. 6). By fitting the overall correlation curves of the washed cells, active transport components are obtained in exactly the same time regime as for cells without inhibitors (Fig. 4B, curve 6). This restoration and the recovery of cell growth show that the inhibition is reversible and does not permanently damage the cells.

DISCUSSION

The stroma of chloroplasts and other plastid types contains water soluble proteins involved in biosynthesis of starch, fatty acids, amino acids, nucleic acids and enzymes used in the assimilation of sulfur and nitrogen. Furthermore, the stroma contains metabolic intermediates, salts, nucleic acids and ribosomes (Hoober, 1984; Kirk and Tilney-Bassett, 1978). In electron microscopic studies the stroma appears crowded, with protein concentrations of up to about 300 mg/ml (Ellis, 1979). Because of the high density of protein and solutes, the stroma is thought to be very viscous. Pulsed nuclear magnetic resonance showed low mobility of water in chloroplasts, suggesting that water molecules in vivo might be bound to macromolecules and therefore highly immobile (Sainis and Srinivasan, 1993). The mobility of water in the stroma is comparable to mobility of water in a 50% bovine serum albumin solution (Sainis and Srinivasan, 1993). Measuring the movement of GFP in the stroma of plastid tubules in tobacco suspension cells by 2PE FCS confirmed the high viscosity of the plastid stroma, but also showed that movement of GFP in the plastid stroma is complex. Table 1 provides a comparison of the modes and velocities with which GFP moves in the cytosol and plastid stroma of tobacco cells compared to the movement in an aqueous solution and in the plasma membrane. GFP moves in the stroma in three different ways: (1) by slow anomalous diffusion of free GFP molecules with a diffusion coefficient in the range of $D=9\pm5\times10^{-9}$ cm^2/second, (2) by active transport of GFP in form of bright batches in the order of 0.12±0.06 μm/second, and (3) by very slow diffusion of the bright batches in the order of $D=10^{-11}$ cm^2/second.

The average diffusion coefficient of free GFP in the plastid stroma, at $9\pm5\times10^{-9}$ cm^2/second, is surprisingly low. Diffusion of GFP in the stroma is anomalous and is about 50 and 100 times slower than diffusion in the cytosol and in an aqueous solution, respectively. Slow and anomalous diffusion could be caused by parameters such as fluid-phase viscosity, i.e. the viscosity in the aqueous space between macromolecules, evanescent binding between macromolecules, and collisional interactions between solutes and macromolecules (Garcia-Perez et al., 1999; Kao et al., 1993; Zimmerman and Minton, 1993). GFP in the plastid stroma has a diffusion coefficient similar to that in membrane-bound proteins, but binding of S65TMGFP4 to the inner envelope membrane is unlikely to be the cause of the slow diffusion because the correlation curves display 3-D diffusion characteristics rather than 2-D diffusion, as would be expected for membrane-bound proteins (Schwille et al., 1999a; Schwille et al., 1999b).

Table 1. Movement of GFP quantified by FCS

			Plastid stromules		
	Aqueous solution	Tobacco cytosol	No inhibitor	FCCP or NaCN	Membrane*
Diffusion (cm^2/second)	$9\pm2.0\times10^{-7}$	$4\pm2.0\times10^{-7}$	$9\pm5\times10^{-9}$‡ 1×10^{-11}§	$9\pm5\times10^{-9}$	$\approx10\times10^{-9}$
Active transport (μm/second)	Not detectable	Not detectable	0.12±0.06	Not detectable	Not detectable

Movement of GFP in the cytosol and plastid stroma of tobacco cells was compared to the movement in an aqueous solution and in the plasma membrane, and to the movement in the plastid stroma of cells treated with FCCP or NaCN.

*Diffusion of GFP fused to a plasma membrane protein in human or rat cell cultures (Schwille et al., 1999a).

‡Diffusion during 'silent' periods without active transport.

§Diffusion during periods with active transport. This movement is not detectable when FCCP or NaCN are present.

The GFP mutant we used, S65TMGFP4, is not responsible for the low diffusion coefficient. S65TMGFP4 has no unusual diffusion characteristics and diffuses like other GFPs such as EGFP (Clontech, Palo Alto, CA) or wild-type GFP with a 6xHis tag, when present in the cytosol of tobacco or in an aqueous solution. Furthermore, the additional 15 amino acids of the mature RECA protein that form the N terminus of the CT-S65TMGFP4 after import into plastids and processing of the leader peptide have little, if any, effect on diffusion. When cells and plastids are lysed and plastid-localized CT-S65TMGFP4 is released into an aqueous solution, the protein shows a diffusion coefficient comparable to S65TMGFP4 in an aqueous solution (data not shown). The diffusion coefficients of EGFP (Schwille et al., 1999a), a His-tagged wild-type GFP (Terry et al., 1995) and of S65TMGFP4, are about 8.7×10^{-7} cm^2/second, 8.7×10^{-7} cm^2/second and $9.0\pm2.0\times10^{-7}$, respectively, in an aqueous solution and 2.7×10^{-7} cm^2/second (Swaminathan et al., 1997) and $4.0\pm2.0\times10^{-7}$ cm^2/second for EGFP and S65TMGFP4 in the cytosol. The diffusion coefficient of S65TMGFP4 in the cytosol of tobacco also fits with the idea that the cytosol is a water-like aqueous solution with some solutes and up to about 200 mg/ml protein (Luby-Phelps, 1994; Swaminathan et al., 1997).

Stromal diffusion of GFP shows anomalous movement, which indicates that GFP does not move freely but is interacting or colliding with other free diffusing molecules or structural components in the plastid stroma. Because GFP in the stroma moves about 100 times slower than GFP in an aqueous solution, it is unlikely that binding to larger protein complexes is solely responsible for slow diffusion. Since the diffusion coefficient for globular molecules scales inversely proportional to the third root of the molecular weight, a freely diffusing particle bound to GFP would need to have a

molecular weight 10^6 times higher, i.e. about 3×10^7 kDa, to induce this slowing down by a factor of 100. Measurements of the time-resolved anisotropy of GFP in the cytosol of human cells using fluorescence microscopy did not show any evidence for binding of GFP to intracellular structures or molecules, which would slow apparent GFP rotation (Swaminathan et al., 1997). Therefore, it is likely that the low mobility of GFP in the plastid stroma is caused by collision and interaction with freely diffusive molecules and by fluid-phase viscosity, with a less likely involvement of binding to freely diffusive larger molecules or to structural elements of the stroma.

As in the plastid stroma, protein density within the mitochondrial matrix is thought to be very high, creating an unusual milieu in which the motion of proteins is severely hindered (Scalettar et al., 1991; Srere, 1980). More recent experiments using fluorescence recovery after photobleaching on GFP-labeled mitochondria in human cells suggest that the mitochondrial matrix is organized into a highly viscous peripheral area with membrane-associated macromolecules and a central region with low protein density and low viscosity in which diffusion is rapid and unrestricted (Partikian et al., 1998). Our measurements on the plastid stroma do not support a separation into a fast and slow diffusing region within a cross section of a plastid tubule; they rather imply that areas with high local concentration of GFP, so-called batches, are mobile and actively transported along the tubule.

GFP is actively transported through plastid tubules

In addition to its movement by diffusion, GFP with 15 amino acids of the mature RECA protein at its N terminus is actively transported through plastid tubules in bright batches. It is unlikely that GFP contains a specific signal that facilitates active transport in the stroma, as GFP is not normally present in plastids and the modified GFP contains only 15 amino acids of a genuine plastid protein. It is more likely that GFP is transported in a nonselective manner. Our data is consistent with a model in which proteins present in certain areas of the plastid form units (batches) that are actively transported through stromules (Fig. 7A,B). Possibly these batches are accumulations of GFP into small vesicles; membrane-bound inclusion bodies have been observed in *Chlamydomonas* chloroplasts (Ketchner et al., 1995).

FCS does not provide information about the direction of the movement nor about the absolute size of the observed GFP batches. The very low diffusion coefficient of 10^{-11} cm^2/second obtained for the batches, as well as their brightness and relatively low number, however, indicate that they consist of larger units of GFP molecules. This is also supported by the occasional observation by epifluorescence microcopy of bright vesicle-like areas that move along stromules (data not shown). In contrast to FCS, which can detect changes on a single molecule scale, direct observation of vesicle movement by CLSM or epifluorescence microscopy requires large differences in the brightness of the fluorescence between vesicles and the surrounding stroma and is therefore usually not observable.

The active transport of GFP through tubules can be separated from diffusion by fitting the correlation curves with mathematical models for active transport and diffusion. The flow model that we assumed for fitting the curves (equations 3, 5) is plug flow rather than laminar flow. Plug flow is characterized by a uniform translation profile of particles within a tube, as one would expect for flow of particles that are large compared to the tube radius, or for active transport along a structure mediated by ATP. Indeed, the active transport contribution can be separated from diffusion by its dependence on ATP. Toxins that deplete the cells of ATP inhibit only the active transport but have no influence on diffusion of single GFP molecules. However, the very slow diffusion of the large batches is no longer observed, which could be interpreted in several ways, as indicated in Fig. 7. Depletion of ATP may suppress the formation of batches (Fig. 7C), the loading of GFP into batches (Fig. 7D), or the movement of batches (Fig. 7E). Using a fixed measurement volume it is difficult to distinguish between these three possibilities. The slight increase of average GFP fluorescence and concentration in tubules of inhibited cells (Fig. 6) seems to support the models in Fig. 7C or D. The absence of the batches, because they do not form or dissolve, as well as a failure to accumulate GFP in batches, would be expected to result in more free GFP and higher fluorescence in stromules (compare Fig. 6). In addition, we would expect to observe a reduction in fluorescence if batches/vesicles that do not contain GFP move through the measuring volume as indicated in (Fig. 7D). However, from the present data, no definite conclusions can be drawn because we did not follow a rise of concentration in one and the same tubule with and without inhibition.

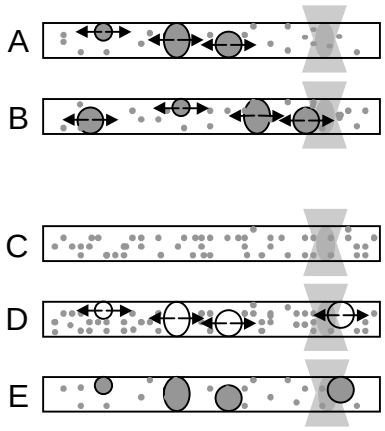

Fig. 7. Model for the movement of GFP and its inhibition in stromules. FCS indicates that GFP moves in different modes through plastid stromules. During periods of dim fluorescence without large fluctuations, small units (single molecules) of GFP simply diffuse through the measured volume (A). During large and slow fluctuation periods, GFP movement is characterized by active flow and diffusion of large batches (perhaps vesicles) of GFP (B). After addition of NaCN or FCCP, active movement and diffusion of large batches ceases, but diffusion of single GFP molecules continues as before. This effect of inhibition of the active movement of GFP through tubules could be explained in several ways: vesicle formation could be prevented (C), loading of GFP into vesicles could be inhibited but empty vesicles might still move (D), the movement of vesicles with GFP could be inhibited (E), or a combination of these possibilities. Stromules are indicated by boxes, vesicles with or without GFP by filled or empty large circles, single GFP molecules by small filled circles, and the movement of vesicles by arrows. For 2PE, only the immediate vicinity of the focal spot, highlighted as an ellipsoid within the laser light double cone, contributes to the signal. Diffusion within the batches or vesicles has been omitted from the model for reasons of clarity.

Advantage of active transport for long-range transport

The observed active transport of GFP through plastid tubules is not very rapid, with an average velocity of about 0.12±0.06 μm/second and a maximum velocity of about 0.4 μm/second. At 0.12 μm/second, a molecule needs about 7 minutes to move through a 50 μm long plastid tubule. For a single molecule, diffusion is faster than the measured active transport for distances up to about 45 μm if a diffusion coefficient of 9×10^{-9} cm^2/second is assumed. Nevertheless, the fluorescence in the actively transported batches is about 10-100 times higher than during the silent periods, suggesting an accumulation of GFP to higher concentrations and in large quantities in the batches. Active transport of large quantities is much more efficient than diffusion. In addition, active transport can create and sustain gradients and transport molecules directionally from one location to another, though our data does not reveal whether or not GFP movement within a tubule is unidirectional. Our FCS data, as well as the observed dynamic nature of stromules, suggests that there may be a hitherto-unknown plastoskeleton that facilitates transport of molecules within plastids. Recently, AtFtsZ, a structural homologue to eukaryotic tubulin, has been found to be involved in plastid division in *Arabidopsis* (Osteryoung et al., 1998). In the future, proteomic analysis of the content of plastids should provide information concerning the possible existence of a plastid network analogous to the cytoskeleton.

Single-cell measurements in vivo with FCS

By applying FCS to single GFP-expressing transgenic plant cells, we were able to obtain estimates of the concentration of the protein in different compartments of the cell, the rate of active transport and the rate of diffusion of the protein. Molecular mobility is essential for processes such as enzymatic reactions, exchange of molecules between and within compartments, signal transduction and metabolic regulation. Though these experiments utilized a GFP fused to merely 15 amino acids of a genuine plastid protein, transgenic organisms can be generated in which GFP is fused to entire proteins in order to compare the mobility of different proteins in different cellular compartments in a variety of types of living cells.

This work was supported by grants to M. R. Hanson from the National Science Foundation (MCB-9808101) and the Energy Biosciences Program of the Department of Energy (DE FG02-89ER14030), and grants to W. W. Webb by the National Science Foundation (DIR8800278) and National Institutes of Health (RR0422 and R07719). P. Schwille received a fellowship from the Alexander von Humboldt Foundation. The FCS experiments were carried out in the NIH-NCRR supported Developmental Resource for Biophysical Imaging Opto-Electronics.

REFERENCES

Brinkmeier, M., Dörre, K., Stephan, J. and Eigen, M. (1999). Two-beam cross-correlation: a method to characterize transport phenomena in micrometer-sized structures. *Anal. Chem.* **71**, 609-616.

Brown, E. B., Wu, E.-S., Zipfel, W. and Webb, W. W. (1999). Measurement of molecular diffusion in solution by multiphoton fluorescence photobleaching recovery. *Biophys. J.* **77**, 2837-2849.

Cao, J., Combs, C. and Jagendorf, A. T. (1997). The chloroplast-located homolog of bacterial DNA recombinase. *Plant Cell Physiol.* **38**, 1319-1325.

Cerutti, H., Osman, M., Grandoni, P. and Jagendorf, A. T. (1992). A homolog of *E. coli* RecA protein in plastids of higher plants. *Proc. Natl. Acad. Sci. USA* **89**, 8068-8072.

Crameri, A., Whitehorn, E. A., Tate, E. and Stemmer, W. P. C. (1996). Improved green fluorescent protein by molecular evolution using DNA shuffling. *Nature Biotechnol.* **14**, 315-319.

Dennis, D. T., Layzell, D. B., Lefebvre, D. D. and Turpin, D. H. (ed.) (1997). *Plant Metabolism.* Harlow: Addison Wesley Longman Ltd.

Ellis, R. J. (1979). The most abundant protein in the world. *Trends Biochem. Sci.* **4**, 241-244.

Elson, E. L. and Magde, D. (1974). Fluorescence correlation spectroscopy. I. Conceptual basis and theory. *Biopolymers* **13**, 1-27.

Feder, T. J., Brust-Mascher, I., Slattery, J. P., Baird, B. and Webb, W. W. (1996). Constrained diffusion or immobile fraction on cell surfaces: a new interpretation. *Biophys. J.* **70**, 2767-2773.

Fuks, B. and Schnell, D. J. (1997). Mechanism of protein transport across the chloroplast envelope. *Plant Physiol.* **114**, 405-410.

García-Pérez, A. I., López-Beltrán, E. A., Klüner, P., Luque, J., Ballesteros, P. and Cerdán, S. (1999). Molecular crowding and viscosity as determinants of translational diffusion of metabolites in subcellular organelles. *Arch. Biochem. Biophys.* **362**, 329-338.

Gillham, N. W. (1994). *Organelle Genes and Genomes*. Oxford: Oxford University Press, Inc.

Grebenok, R. J., Pierson, E. A., Lambert, G. M., Gong, F.-C., Afonso, C. L., Haldemann-Cahill, R., Carrington, J. C. and Galbraith, D. W. (1997). Green-fluorescent protein fusions for efficient characterization of nuclear localization signals. *Plant J.* **11**, 573-586.

Haseloff, J., Siemering, K. R., Prasher, D. C. and Hodge, S. (1997). Removal of a cryptic intron and subcellular localization of green fluorescent protein are required to mark transgenic *Arabidopsis* plants brightly. *Proc. Natl. Acad. Sci. USA* **94**, 2122-2127.

Heytler, P. G. and Prichard, W. W. (1962). A new class of uncoupling agents – carbonyl cyanide phenylhydrazones. *Biochem. Biophys. Res. Commun.* **7**, 272-275.

Hoober, K. J. (1984). *Chloroplasts*. New York, London: Plenum Press.

Kao, H. P., Abney James, R. and Verkman, A. S. (1993). Determinants of the translational mobility of a small solute in cell cytoplasm. *J. Cell Biol.* **120**, 175-184.

Keegstra, K. and Cline, K. (1999). Protein import and routing systems of chloroplasts. *Plant Cell* **11**, 557-570.

Ketchner, S. L., Drapier, D., Olive, J., Gaudriault, S., Girard, B. J. and Wollman, F. A. (1995). Chloroplasts can accommodate inclusion bodies: evidence from a mutant of *Chlamydomonas reinhardtii* defective in the assembly of the chloroplast ATP synthase. *J. Biol. Chem.* **270**, 15299-15306.

Kirk, J. T. O. and Tilney-Bassett, R. A. E. (1978). *The Plastids: Their Chemistry, Structure, Growth, and Inheritance*. Amsterdam, New York: Elsevier/North Holland Biomedical Press.

Köhler, R.H. (1998). GFP for *in vivo* imaging of subcellular structures in plant cells. *Trends Plant Sci.* **3**, 317-320.

Köhler, R. H., Cao, J., Zipfel, W. R., Webb, W. W. and Hanson, M. R. (1997a). Exchange of protein molecules through connections between higher plant plastids. *Science* **276**, 2039-2042.

Köhler, R. H., Zipfel, W. R., Webb, W. W. and Hanson, M. R. (1997b). The green fluorescent protein as a marker to visualize plant mitochondria *in vivo*. *Plant J.* **11**, 613-621.

Köhler, H. R. and Hanson, R. M. (2000). Chloroplast-tubules of vascular plants are tissue-specific and developmentally regulated. *J. Cell Sci*. **113,** 81-89.

Koppel, D. E., Axelrod, D., Schlessinger, J., Elson, E. L. and Webb, W. W. (1976). Dynamics of fluorescence marker concentration as a probe of mobility. *Biophys. J.* **16**, 1315-1330.

Luby-Phelps, K. (1994). Physical properties of cytoplasm. *Curr. Opin. Cell Biol.* **6**, 3-9.

Magde, D., Elson, E. L. and Webb, W. W. (1972). Thermodynamic fluctuations in a reacting system – measurement by fluorescence correlation spectroscopy. *Phys. Rev. Lett.* **29**, 705-708.

Magde, D., Elson, E. L. and Webb, W. W. (1974). Fluorescence correlation spectroscopy. II. An experimental realization. *Biopolymers* **13**, 29-61.

Magde, D., Elson, E. L. and Webb, W. W. (1978). Fluorescence correlation spectroscopy. III. Uniform translation and laminar flow. *Biopolymers* **17**, 361-376.

Ohlrogge, J. B. and Jaworski, J. G. (1997). Regulation of fatty acid synthesis. In *Annual Review of Plant Physiology and Plant Molecular*

Biology, Vol. 48 (ed. R. L. E. Jones), pp. 109-136. Palo Alto, USA: Annual Reviews Inc.

Osteryoung, K. W., Stokes, K. D., Rutherford, S. M., Percival, A. L. and Lee, W. Y. (1998). Chloroplast division in higher plants requires members of two functionally divergent gene families with homology to bacterial *ftsZ*. *Plant Cell* **10**, 1991-2004.

Partikian, A., Olveczky, B., Swaminathan, R., Li, Y. and Verkman, A. S. (1998). Rapid diffusion of green fluorescent protein in the mitochondrial matrix. *J. Cell Biol.* **140**, 821-829.

Sainis, J. K. and Srinivasan, V. T. (1993). Effect of the state of water as studied by pulsed NMR on the function of RUBISCO in a multienzyme complex. *J. Plant Physiol.* **142**, 564-568.

Scalettar, B. A., Abney, J. R. and Hackenbrock, C. R. (1991). Dynamics, structure, and function are coupled in the mitochondrial matrix. *Proc. Natl. Acad. Sci. USA* **88**, 8057-8061.

Schwille, P., Bieschke, J. and Oehlenschlaeger, F. (1997). Kinetic investigations by fluorescence correlation spectroscopy: The analytical and diagnostic potential of diffusion studies. *Biophys. Chem.* **66**, 211-228.

Schwille, P., Haupts, U., Maiti, S. and Webb, W. W. (1999a). Molecular dynamics in living cells observed by fluorescence correlation spectroscopy with one- and two-photon excitation. *Biophys. J.* **77**, 2251-2265.

Schwille, P., Korlach, J. and Webb, W. W. (1999b). Fluorescence correlation spectroscopy with single molecule sensitivity on cell and model membranes. *Cytometry* **36**, 176-182.

Srere, P. A. (1980). The infrastructure of the mitochondrial matrix. *Trends Biochem. Sci.* **5**, 120-121.

Swaminathan, R., Hoang, C. P. and Verkman, A. S. (1997). Photobleaching recovery and anisotropy decay of green fluorescent protein GFP-S65T in solution and cells: Cytoplasmic viscosity probed by green fluorescent protein translational and rotational diffusion. *Biophys. J.* **72**, 1900-1907.

Temple, S. J. and Sengupta-Gopalan, C. (1997). Manipulating amino acid biosynthesis. In *A Molecular Approach to Primary Metabolism in Higher Plants* (ed. C. H. Foyer and W. P. Quick), pp. 155-177. London: Taylor & Francis.

Terry, B. R., Matthews, E. K. and Haseloff, J. (1995). Molecular characterisation of recombinant green fluorescent protein by fluorescence correlation microscopy. *Biochem. Biophys. Res. Commun.* **217**, 21-27.

Thompson, N. L. (1991). Fluorescence correlation spectroscopy. In *Topics in Fluorescence Spectroscopy*, Vol. 1 (ed. J. R. Lakowicz), pp. 337-378. New York: Plenum Press.

Tobin, A. K. (1992). *Plant Organelles: Compartmentation of Metabolism in Photosynthetic Cells*. Cambridge, New York: Cambridge University Press.

Tzagoloff, A. (1982). *Mitochondria*. New York, London: Plenum Press.

Yokoe, H. and Meyer, T. (1996). Spatial dynamics of GFP-tagged proteins investigated by local fluorescence enhancement. *Nature Biotechnol.* **14**, 1252-1256.

Zimmerman, S. B. and Minton, A. P. (1993). Macromolecular crowding: Biochemical, biophysical, and physiological consequences. In *Annual Review of Biophysics and Biomolecular Structure*, Vol. 22 (ed. D. M. Engelman), pp. 27-65. Palo Alto: Annual Reviews Inc.